

Characterization of asphaltic oil occurrences from the south-eastern margin of the Basque-Cantabrian Basin, Spain

P. MARÍN¹ G. MÁRQUEZ² J.R. GALLEGO³ A. PERMANYER^{1,*}

¹Department de Geologia, Petrologia i Prospecció Geològica, Universitat de Barcelona
C/ Martí i Franquès s/n, 08028-Barcelona, Spain. Permanyer E-mail: albert.permanyer@ub.edu
Marín E-mail: p.marinbarba@gmail.com

²Departamento de Ingeniería Minera, Mecánica y Energética, Universidad de Huelva
C/ La Rábida s/n, 21819-Huelva, Spain. E-mail: gonzalo.marquez@diq.uhu.es

³Departamento de Explotación y Prospección de Minas, Universidad de Oviedo
C/ Gonzalo Gutiérrez Quirós, 33600-Mieres, Spain. E-mail: jgallego@uniovi.es

*Corresponding author.

ABSTRACT

A geochemical investigation has been undertaken on biodegraded hydrocarbons in outcropping reservoirs of the south-eastern margin of the Basque-Cantabrian Basin (Álava sector). The aims of the study were the characterization of the geochemical features and biodegradation level of these hydrocarbons, and the evaluation of their resemblance to oils from the Ayoluengo onshore oil field by means of isotopic analyses and gas chromatography-mass spectrometry techniques. Most of the samples lack *n*-alkanes, isoprenoids, low molecular weight aromatic compounds, steranes, homohopanes, diasteranes and triaromatic steroids, whereas hexacyclic and heptacyclic alkanes appear as key compounds although some structures were not totally elucidated. Thermal maturity has been assessed with several parameters and a calculated-equivalent vitrinite reflectance value of around 0.8% was estimated. In addition, gammacerane content, diasterane-to-sterane ratio and C₃₅ to C₃₄ hopanes ratio suggest that the Álava oil shows were derived from a carbonate rock deposited in a reducing, water-stratified and possibly hypersaline environment. Isotopic signatures and other data confirmed that these hydrocarbons are not genetically related to the oils from Ayoluengo and, consequently, their origin is associated with a yet unknown source rock in the basin.

KEYWORDS | Asphaltic oil occurrences. Basque-Cantabrian Basin. Álava sector. Ayoluengo oil field. Biodegradation.

INTRODUCTION

The Basque-Cantabrian Basin currently constitutes the only location with onshore hydrocarbon production within the Iberian Peninsula. The basin covers a wide onshore and offshore area and is located between the Paleozoic Basque and Asturian massifs in the East and

West, respectively, the Tertiary Ebro and Duero basins in the South and the Bay of Biscay in the North (Fig. 1A). This northern Spanish Mesozoic-Cenozoic basin was folded and thrustured during the Pyrenean orogeny and its present structure consists of a north and south verging thrust belt. Detailed structural and stratigraphic descriptions of the Basque-Cantabrian Basin have been

reported by several authors (Ramírez del Pozo, 1969; Pujalte, 1977; Salamon, 1982; Rat, 1988; Grafe and Wiedmann, 1993; Cámara, 1997; Gómez *et al.*, 2002; Capote *et al.*, 2002; Barnolas and Pujalte, 2004).

In the 1960s, occurrence of Lower Cretaceous tar sands in the south-western part of the Basque-Cantabrian Basin led to the discovery of the Ayoluengo onshore oil field. Its structure consist of a Late Jurassic–Early Cretaceous salt-related extensively faulted anticline, whose main reservoirs are Upper Jurassic–Lower Cretaceous siliciclastic sandstone beds with porosities ranging from 15% to 25% and permeabilities up to 1000mD (Sanz, 1967; Álvarez de Buergo and García, 1996; Quesada *et al.*, 1997). Geochemical studies focusing on biomarker oil-to-source rock correlations (Quesada *et al.*, 1997; Beroiz and Permanyer, 2011) showed that the Ayoluengo oil is derived from a Pliensbachian–Toarcian shale source rock. These Lower Jurassic organic-rich shales stand out in the whole Liassic sequence by having total organic carbon (TOC) content around 4%, high Rock-Eval S2 values ($S2 \leq 21$ mg HC per gram of rock) and hydrogen indices (HI) greater than 400mg HC per gram of organic carbon (Quesada *et al.*, 1997; Quesada *et al.*, 2005; Beroiz and Permanyer, 2011). Similar facies have also been reported in the North Sea and the Paris Basin and proved there as effective source rocks (Cooper and Barnard, 1984; Herron and Le Tendre, 1990; Huc, 1990). Additionally, $\delta^{13}C$ isotopic studies suggest that Lower Cretaceous tar sands outcropping near the Ayoluengo oil field (*e.g.* Basconcillos del Tozo and Zamanzas locations) have the same origin as the Ayoluengo oil (Beroiz and Permanyer, 2011).

Furthermore, oil shows are common throughout the Basque-Cantabrian Basin. For instance, pyrobitumens in Albian carbonates in the northern margin of the basin have been studied by Agirrezabala *et al.* (2008), who concluded that they correlate with a previously unrecognised source rock in the basin, *i.e.*, the Middle Albian–Lower Cenomanian Black Flysch Group (mid-Cretaceous), whose TOC content is around 1%.

In the south-eastern part of the Basque-Cantabrian Basin (Álava sector) bitumen-impregnated Upper Cretaceous Campanian and Maastrichtian carbonates and sands occur, outcropping beside Triassic diapiric structures. Studies of these hydrocarbons were carried out by Dorronsoro *et al.* (1994) and García Sánchez (1994), though no correlation with the western hydrocarbons of the basin has been carried out until now. Therefore, this paper reports on hydrocarbons sampled in exhumed reservoirs near the Maestu and Peñacerrada diapirs in order to: i) characterize their biodegradation and maturity level, ii) suggest a depositional environment and source rock, and,

above all, iii) to determine their genetic resemblance to hydrocarbons of the Ayoluengo oil field. For this purpose, a geochemical study including quantification of saturated and aromatic hydrocarbons, as well as resins and asphaltenes (SARA), stable carbon isotope analyses and gas chromatography-mass spectrometry have been carried out.

GEOLOGICAL SETTING

The origin and evolution of the Basque-Cantabrian Basin is linked to the Permo–Triassic and Late Jurassic–Early Cretaceous rifting cycles, the latter being associated with the opening of the North Atlantic and the Bay of Biscay. Its present structure is also a result of the Pyrenean compression (Late Eocene to Miocene), in which Keuper evaporites acted as the detachment level promoting the formation of diapirs, which are abundant in the central and eastern part of the Basque-Cantabrian Basin.

After predominant sedimentation of clays and evaporites during Keuper times, subsidence in the basin led to a Jurassic marine transgression which formed a fairly uniform platform deposit: the Liassic–Dogger macrosequence, characterized by shallow facies such as Sinemurian shallow-marine carbonates, Pliensbachian to Toarcian organic-rich marls and shales or mid-Jurassic interbedded lime mudstones and marls (Beroiz and Permanyer, 2011). In Late-Jurassic and until Aptian–Albian, a second rifting cycle took place that ended with the oceanic crust creation in the central part of the Bay of Biscay (Roest and Srivastava, 1991; Alonso *et al.*, 2007). Within this area, syn-rift sequences are basically clastic. During Cenomanian and Santonian times, a widespread marine transgression occurred and depositional facies consisted of shallow-marine carbonates and shales. Compression associated with the Pyrenean orogeny firstly took place in Late Santonian and led to a gradual uplift and the onset of a marine regression (Maastrichtian), when very shallow marine carbonates, dolomite and evaporites were deposited (Portero and Ramírez, 1979; Grafe and Wiedmann, 1993). Main orogeny phases responsible for the current-day-observed fold-and-thrust topography and diapirism occurred during Late Eocene and Miocene times (Alonso *et al.*, 2007). Paleocene to Early Oligocene deposits consist of continental to lacustrine sediments whilst Late Oligocene to Miocene sedimentation is mainly clastic and occurred as post-orogenic molasse (Alonso-Zarza *et al.*, 2002).

The main study area is located in the south-eastern margin of the Basque-Cantabrian Basin, between the Miranda–Treviño–Urbasa syncline and the Cantabrian Ranges (Fig. 1B). Within this area, the deformation

is mainly located in the aforementioned ranges, highly folded and thrust. The Miranda–Treviño–Urbasa syncline (ENE–WSW) is locally affected by the Maestu diapir. Besides the Maestu and Peñacerrada diapirs, gravimetric studies reveal a non-outcropping diapir near Santa Cruz de Campezo (Carreras-Suárez and Ramírez del Pozo, 1978). Associated with these diapirs, Late Cretaceous (Campanian and Maastrichtian) materials are bitumen-impregnated.

METHODS

Samples

Six asphaltic oil samples were collected from three different outcrops in the south-eastern part of the Basque-Cantabrian Basin (see Fig. 1B). Maestu-1 and Maestu-7 samples are grainstones with micro- and macro-foraminifera, echinoderms and bivalves. Atauri-3 is a

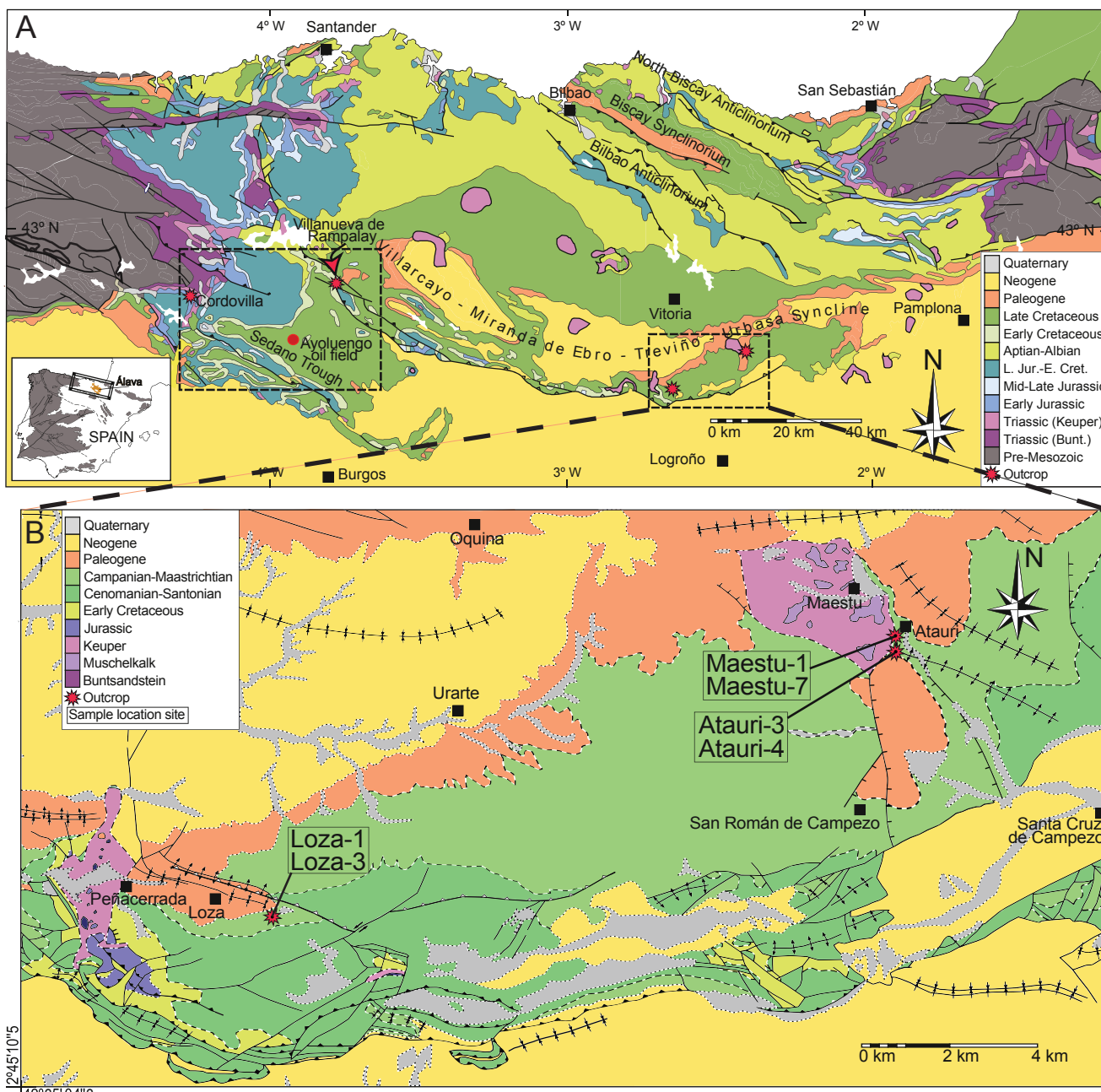


FIGURE 1. A) Geological map of the Basque-Cantabrian Basin (modified from Ábalos *et al.*, 2008). Two sampled areas, referred in the text as the eastern sector (Álava) and the western sector are marked; B) Geological map of the main study zone (Álava sector, south-eastern Basque-Cantabrian Basin).

packstone with foraminifera, bryozoans and red algae, and abundant rock fragments. Atauri-4 is a wackestone of foraminifera with detrital quartz and bryozoans. Loza-1 is a matrix-supported lithic arenite with quartz, sandstone and dolomite rock fragments, detrital quartz, feldspar and echinoderms. Loza-3 is a grainstone with bryozoans, red algae and abundant detrital quartz and quartzite (Marín, 2012). Two Lower Cretaceous oil shows (Rampalay-1 and Rampalay-2) outcropping in the south-western part of the Basque-Cantabrian Basin (see Fig. 1a) have also been sampled. Lastly, other data (Beroiz and Permanyer, 2011; Permanyer *et al.*, 2013) have been used in this study, namely: i) gas chromatography-mass spectrometry (GC-MS) profiles of the saturated hydrocarbons of the Jurassic (Pliensbachian–Toarcian) source rock outcropping in Cordovilla (south-western part of the Basque-Cantabrian Basin; see Fig. 1a) and ii) stable carbon isotope results of two oils from the Ayoluengo field (AYO-32 and AYO-38).

All samples were dehydrated with warm toluene (ASTM D1796 standard method; American Society for Testing and Materials, 2004). An aliquot of each sample was fractionated into saturated and aromatic hydrocarbons, resins and asphaltenes compounds (SARA method; Bennett and Larter, 2000).

Saturated and aromatic hydrocarbons were analysed by gas chromatography-mass spectrometry (GC-MS). The GC-MS analyses were performed on a Thermo Scientific Trace GC Ultra gas chromatograph with a DB-5 Agilent Technologies column (60m × 0.25mm i.d. × 0.1µm film) coupled to a ITQ900 mass spectrometer. Samples were injected using a splitless injector at 280°C, and helium was used as a carrier gas with a constant flow rate of 1ml/min. The oven temperature was programmed to run from

an initial temperature of 40°C (held for 1min) to a final temperature of 300°C at 2°C/min, and then held at 300°C for 60min. The mass spectrometer was operated in selective ion monitoring (SIM) electron impact mode (electron input energy, 40eV; source temperature, 200°C). Ions at *m/z* 57, 84, 123, 177, 183, 191, 205, 217, 231 and 259 (saturated fraction) and *m/z* 142, 156, 170, 178, 184, 192, 198, 206, 231 and 253 (aromatic fraction) were scanned with a dwell time of 0.1s. Data were acquired with Xcalibur software.

GC-MS full scan analyses of selected samples were carried out on a Shimadzu QP2010 gas chromatograph-mass spectrometer with a DB-5 Agilent Technologies column (60m × 0.25mm i.d. × 0.1µm film). GC conditions are the same to those described above. The mass spectrometer was operated in full scan electron impact mode (electron input energy, 40eV; source temperature, 200°C). Data were analyzed with Shimadzu software.

Carbon isotopic determination on whole oil and SARA fractions was performed using a Thermo Finnigan1112 elemental analyzer coupled to a Finnigan Mat Delta C mass spectrometer. The reference materials were USGS-40 L-glutamic acid, IAEA-CH6 saccharose, IAEA-CH7 polyethylene, IAEA 600caffeine, and acetanilide. The ¹³C/¹²C ratio is reported in “δ” notation and δ¹³C refers to PDB (pee dee belemnite).

Ni and V concentrations were determined on all samples using an energy-dispersive X-ray Analytical Axios spectrometer. Also, isolation, purification, and HPLC analyses of ETIO VO-porphyrins and vanadyl-DPEP followed the procedure of Sundararaman (1985). Finally, a hierarchical cluster analysis based on isotopic data and other parameters was performed using the SPSS 18.0 package for Windows.

TABLE 1. SARA fractioning (wt.%), V-to-Ni and carbon isotopic values (‰) for the eastern oil shows (Atauri, Loza and Maestu) and western hydrocarbons (Rampalay tar sands and Ayoluengo oils)

Sample	Saturates	Aromatics	Resins	Asphaltenes	δ ¹³ C _{sat}	δ ¹³ C _{aro}	δ ¹³ C _{res}	δ ¹³ C _{asp}	δ ¹³ C _{whole oil}	Ni (ppm)	V/(Ni+V)
Atauri-3	7.38	22.45	9.08	61.09	-28.3	-25.84	-26.02	-26.34	-26.24	12	0.45
Atauri-4	10.8	16.48	7.7	65.02	-28.11	-25.8	-25.81	-26.34	-26.05	10	0.46
Loza-1	11.87	37.88	13.78	36.46	-27.79	-25.77	-25.85	-26.02	-25.5	8	0.43
Loza-3	7.77	17.86	8.16	66.21	-27.8	-25.77	-25.96	-26.01	-25.99	7	0.43
Maestu-1	12.18	30.69	11.67	45.46	-28.16	-25.66	-25.85	-26.36	-26.17	13	0.45
Maestu-7	13.24	27.51	14.03	45.21	-28.2	-25.76	-25.76	-26.29	-24.44	10	0.44
Rampalay-1	36.01	31.59	19.78	12.62	-29.67	-29.02	-29.32	-29.47	-29.44	-	-
Rampalay-2	32.81	13.12	21.73	32.34	-29.71	-28.99	-29.25	-29.6	-29.46	-	-
Ayoluengo-32 ^a	-	-	-	-	-30.11	-29.32	-29.51	-29.31	-29.99	0.13	0.68
Ayoluengo-38 ^a	-	-	-	-	-29.87	-29.12	-29.53	-28.96	-29.98	0.12	0.67

^aData from Permanyer *et al.* (2013)

RESULTS AND DISCUSSION

Asphaltic oil characteristics

Bulk geochemical data

Table 1 shows the bulk vanadium and nickel composition of all the samples from the Álava sector. Group type analyses (SARA fractions expressed as weight percentage) indicate that the six samples have a similar composition: 16.48–37.88% of aromatics (average 25.5%), saturated hydrocarbons not exceeding 13.24%, and a polar fraction ranging between 50.25 and 74.37%. Thus, these oil shows consist of “heavy or degraded oils” according to Tissot and Welte (1984). All samples show asphaltene percentages (up to 66.21%) significantly higher than resin contents.

Hydrocarbons extracted from Rampalay-1 and Rampalay-2 tar sands show percentages of saturated hydrocarbons (around 34%, see Table 1) slightly higher than those of the samples from Álava, and they both can be classified as “aromatic oils” (Tissot and Welte, 1984). In addition, these two tar sands show resin percentages slightly higher, and asphaltene contents lower than those of the six eastern asphaltic oil materials.

Samples from Álava show similar $V/(Ni+V)$ ratios (approximately 0.45) and Ni concentrations close to 10ppm. $V/(Ni+V)$ ratios averaging 0.67 have been previously reported for Ayoluengo oils (Permanyer *et al.*, 2013).

Carbon isotopic data

The similar isotopic compositions of the six asphaltic oils from the Álava sector (whole oil, saturates, aromatics, resins and asphaltenes; Fig. 2) suggests that these oil shows were all derived from the same source rock. The $\delta^{13}C$ signature of Rampalay tar sands is almost identical to the isotopic composition of the Ayoluengo oils (Beroiz and Permanyer, 2011). These two tar sands are isotopically lighter (about 3‰) than the six samples from the eastern part of the Basque-Cantabrian Basin. Standard deviations are close enough to analytical error (0.5‰). Although carbon isotopic differences up to 3‰ can be explained by biodegradation and maturation processes (Peters *et al.*, 2005), other evidences could suggest that these differences may be caused by the existence of two groups of genetically related oil shows.

As shown in the Sofer diagram (Sofer, 1984; Fig. 2B), the six samples from the Álava sector are located on the terrigenous organic matter line. In contrast, $\delta^{13}C$ values for the oils and tar sands from the western part of the Basque-Cantabrian Basin indicate a marine source organic

matter (Beroiz and Permanyer, 2011). Nevertheless, it is noteworthy that biodegradation may alter carbon isotopic signature towards less negative $\delta^{13}C$ values (Sofer, 1984; Peters *et al.*, 2005; Galimov, 2006). Such isotopic shift in the non-polar fractions is sometimes negligible (Mansuy

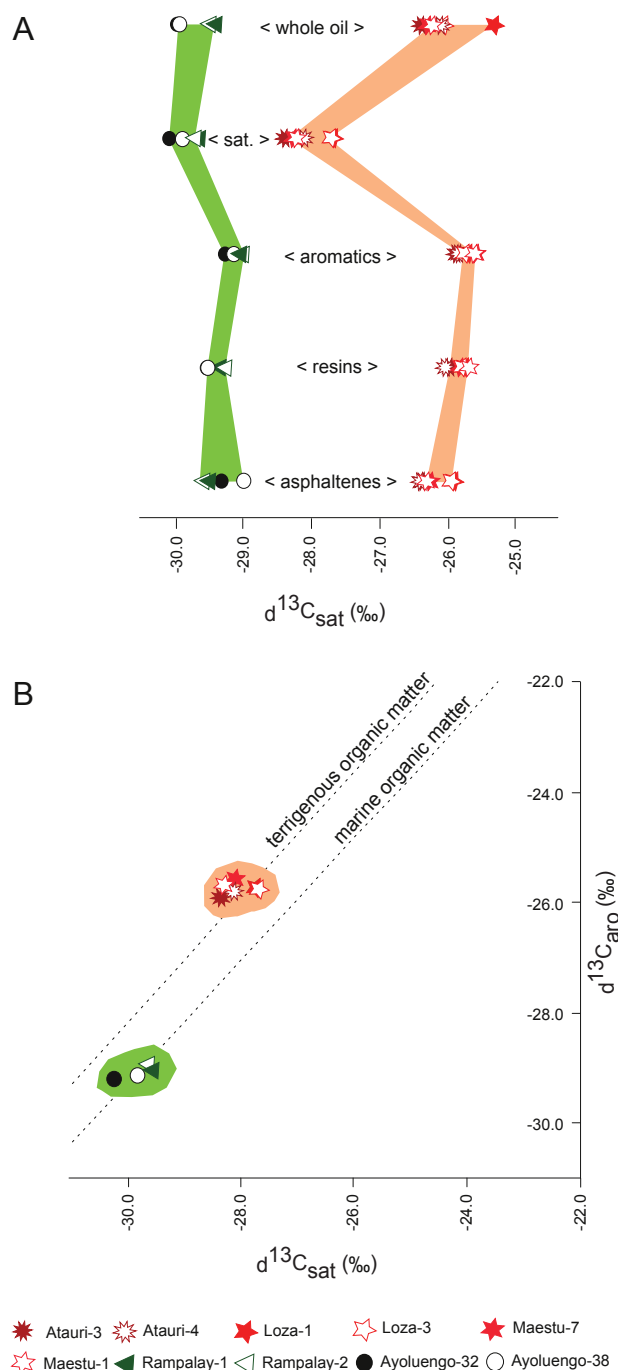


FIGURE 2. Stable carbon isotope diagrams showing the comparison between the eastern hydrocarbons (Atauri, Maestu and Loza oil shows) and the western hydrocarbons (Rampalay tar sands and Ayoluengo oils). A) Galimov–Stahl’s diagram; B) Sofer’s diagram. Note: “Sat” (saturates), “Aro” (aromatics).

et al., 1997; Meckenstock *et al.*, 1999) or may be up to 4‰ (Galimov and Frik, 1985). The two similar and biodegraded Rampalay samples (as discussed below) have shifts lower than 0.5‰ when compared with the unaltered Ayoluengo oils. For the samples from the eastern part of the Basque-Cantabrian Basin, as their source rock is yet to be determined, the due-to-biodegradation shift is unknown.

Saturated hydrocarbons

Gas chromatographic analyses of saturates show a lack of *n*-alkanes and isoprenoids in each of the six asphaltic oil materials from Álava and both tar sands from Rampalay (Fig. 3). Tricyclopolyrenanes can be observed in all the samples from the Álava sector, whereas hopanoids appear to be partly (Loza-1, Loza-3 and Maestu-7) or almost completely removed (Maestu-1 and Atauri-3). Also, a high abundance of gammacerane compared to other triterpanes is observed in some of the samples (Fig. 4A). 18 α (H)-22,29,30 trisnorhopane (Ts) and 17 α (H)-22,29,30 trisnorhopane (Tm) are unaltered or only slightly affected in Loza-1, Loza-3 and Maestu-7, but both biomarkers are not present in Maestu-1 or Atauri-3. Rampalay-1 and Rampalay-2 have a common *m/z* 191 mass chromatogram profile (Fig. 4a), showing distinctive Ts/Tm and C₃₅22S/C₃₄22S hopanes ratios when comparing to Atauri-4.

C₂₇ and C₂₈ regular sterane homologues appear to be highly degraded in Loza-1 and Loza-3, whereas C₂₉ homologues and C₂₇ diasteranes appear to be only partially removed and near-intact, respectively. No preference for any isomer or stereoisomer is observed. C₃₀ steranes and pregnanes remain unaltered in these two similar samples (Fig. 4B). In contrast, C₂₇, C₂₈, and C₂₉ regular steranes are absent in Atauri-3, Atauri-4, Maestu-1, and Maestu-7, which can indicate more severe surface biodegradation processes (Seifert *et al.*, 1984). However, tar sands from the south-western Basque-Cantabrian Basin and the Jurassic source-rock from Cordovilla can be characterized by the C₂₇>C₂₈>C₂₉ pattern of regular steranes and the near-absence of pregnanes (see Fig. 4B), whereas 20S and 20R isomers of 13 β (H),17 α (H)-diacholestane appear to be abundant in these three asphaltic oil materials.

Gas chromatograms of saturates of samples from Álava reveal several rare peaks with retention times similar to those of extended hopanes appear as well (see Figs. 3 and 4A). In fact, the *m/z* 191 and 217 mass chromatograms exhibit clear signals that may correspond to several hexacyclic and heptacyclic alkanes. Though these hydrocarbon compounds are dominant in Atauri-3, Atauri-4, Maestu-1 or Maestu-7 and may have been unmasked with biodegradation, they are also present in Loza-1 and Loza-3. On the contrary, these hexacyclic and heptacyclic alkanes are not present in Rampalay-1, Rampalay-2, and the Cordovilla source rock

(see Fig. 4a). GC-MS full scan analyses have led to identify these latter alkanes as a series of C₃₃ to C₃₉ hexacyclic and C₃₆ to C₃₈ heptacyclic alkanes (Table 2).

The C₃₃ to C₃₅ homologues of the hexacyclic alkanes have been reported previously by Dorronsoro *et al.* (1994). In addition, C₃₃–C₃₆ hexacyclic and C₃₇–C₄₀ heptacyclic alkanes have also been observed in the ostracode zone-sourced oils from the Western Canada sedimentary basin (Li *et al.*, 1996), and they are thought to derive from a restricted, brackish to freshwater environment. Series of C₃₃–C₄₃ hexacyclic and heptacyclic alkanes have also been identified in carbonate source rocks in the Aquitaine Basin (Poinsot *et al.*, 1995).

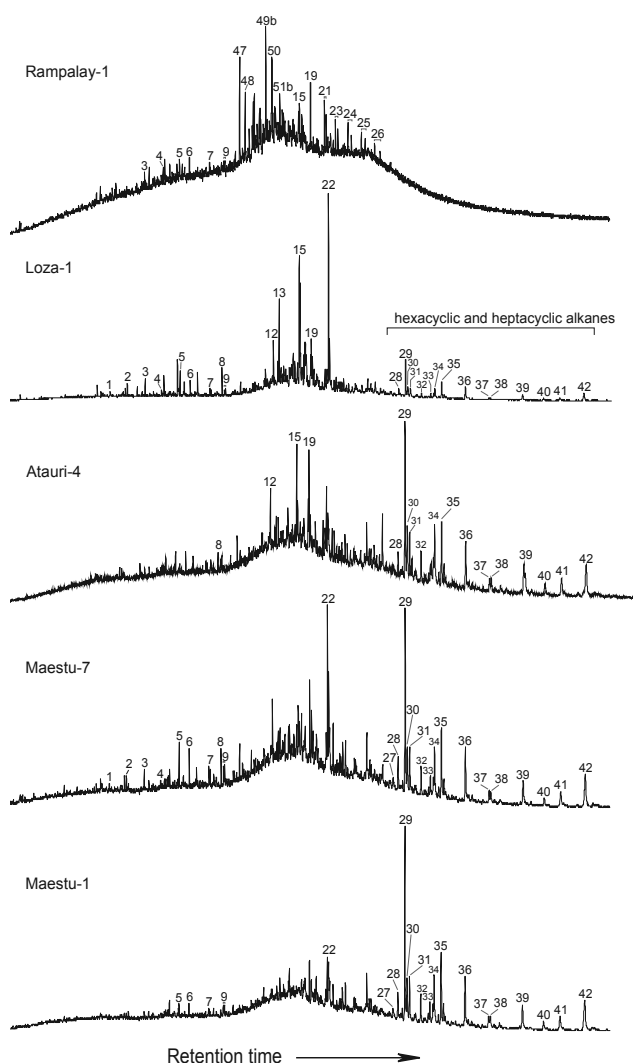


FIGURE 3. Gas chromatograms of the saturated fractions of the western tar sands (Rampalay-1) and three progressively more biodegraded eastern oil shows (Loza-1, Atauri-4, Maestu-7 and Maestu-1). Compounds are listed in the Appendix.

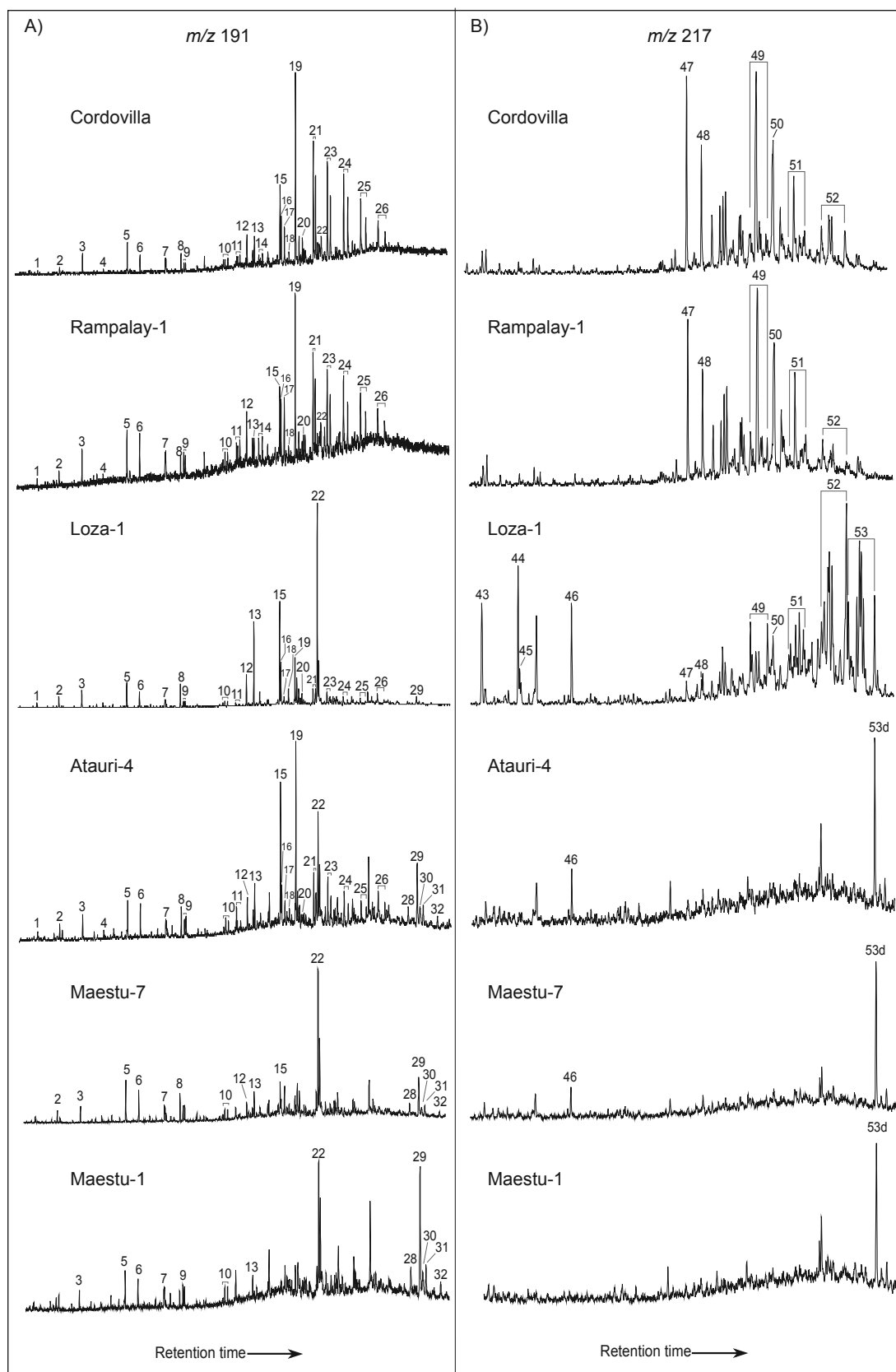


FIGURE 4. Mass fragmentograms of western hydrocarbons (Cordovilla source rock and Rampalay-1 tar sand) and eastern hydrocarbons (Loza-1, Atauri-4, Maestu-7 and Maestu-1 oil shows). A) Triterpanes mass fragmentograms (m/z 191); B) Steranes mass fragmentograms (m/z 217). Compounds are listed in the Appendix.

TABLE 2. List of hexacyclic and heptacyclic alkanes identified in the samples from the eastern Basque-Cantabrian Basin

Compound No.	Empirical Formula	M ⁺	Major diagnostic ions ^a
27	C ₃₃ H ₅₆ hexacyclic alkane	452(42)	191(52), 203(77), 259(41), 271(27), 313(31), 437(29)
28	C ₃₃ H ₅₆ hexacyclic alkane	452(28)	191(50), 203(92), 259(47), 271(49), 355(10), 437(21)
29	C ₃₄ H ₅₈ hexacyclic alkane	466(30)	191(57), 217(96), 259(55), 285(65), 327(17), 451(19)
30	C ₃₄ H ₅₈ hexacyclic alkane	466(26)	191(100), 217(70), 259(43), 285(27), 355(13), 451(8)
31	C ₃₄ H ₅₈ hexacyclic alkane	466(27)	191(71), 217(100), 259(42), 285(64), 327(19), 451(26)
32	C ₃₄ H ₅₈ hexacyclic alkane	466(22)	191(26), 217(69), 259(23), 285(28), 327(29), 451(26)
33	C ₃₅ H ₆₀ hexacyclic alkane	480(11)	191(43), 231(100), 259(44), 299(39), 327(30), 355(33)
34	C ₃₅ H ₆₀ hexacyclic alkane	480(20)	191(45), 207(32), 231(83), 259(48), 299(26), 327(21)
35	C ₃₅ H ₆₀ hexacyclic alkane	480(30)	191(63), 231(85), 259(55), 299(34), 327(16), 395(18), 465(29)
36	C ₃₆ H ₆₂ hexacyclic alkane	494(22)	191(31), 245(39), 259(37), 327(14), 395(72), 479(17)
37	C ₃₇ H ₆₄ hexacyclic alkane	508(23)	191(100), 207(46), 259(85), 327(33), 395(95), 493(37)
38	C ₃₆ H ₆₀ heptacyclic alkane	492(28)	191(58), 205(11), 259(19), 281(100), 311(33), 341(50), 477(30)
39	C ₃₈ H ₆₆ hexacyclic alkane	522(36)	191(37), 205(41), 259(27), 273(31), 327(25), 395(100)
40	C ₃₉ H ₆₈ hexacyclic alkane	536(13)	191(30), 207(58), 259(24), 281(50), 395(81), 521(33)
41	C ₃₇ H ₆₂ heptacyclic alkane	506(27)	191(56), 205(15), 259(59), 331(34), 491(18)
42	C ₃₈ H ₆₄ heptacyclic alkane	520(35)	191(40), 203(75), 259(55), 271(79), 339(35), 505(30)

^aRelative intensity is given in brackets.

Aromatic hydrocarbons

Gas chromatographic analyses of the aromatic fraction show a lack of low molecular weight compounds and an unresolved hump in each of the six oil shows from the Álava sector (Fig. 5).

Triaromatic steroid distributions have been clearly identified in Rampalay-1, Rampalay-2, Loza-1, and Loza-3. Monoaromatic steroids have not been detected in Maestu-1 or Atauri-3. However, the presence of monoaromatic diasteroids has been observed in these latter two samples. Also, all samples from Álava display several peaks eluting at higher retention times. GC-MS full scan has led to identify these latter peaks as a series of C₃₁ to C₃₄ diaromatic hydrocarbons (Fig. 5). On the contrary, the two Rampalay tar sands do not exhibit the signals of these diaromatic compounds. Figure 6 shows the representative mass spectra of the aforementioned series of hexacyclic and heptacyclic alkanes, as well as of the series of diaromatic hydrocarbons.

Biodegradation

Thermal maturity and source determination of organic matter in oil shows can be problematic given that biomarkers may be affected by biodegradation (Bennett

and Larter, 2006). The six samples from the eastern Basque-Cantabrian Basin have been heavily altered by biodegradation. All the samples show a lack of *n*-alkanes, isoprenoids, phenanthrenes, and dibenzothiophenes, among others. 25-norhopanes were not detected in these six samples and, consequently, can be stated that steranes were biodegraded earlier than hopanes, thereby suggesting surface biodegradation (Peters *et al.*, 2005).

The near-total absence of C₂₇ to C₂₈ regular steranes and the partial depletion of C₂₉ homologues in Loza-1 and Loza-3 samples indicate a biodegradation level between 6 and 7 according to the Peters and Moldowan scale (Peters *et al.*, 2005). In these two oil shows, pentacyclic triterpanes are partially - C₂₉ and C₃₀ 17 α -hopanes - or completely - extended hopanes - depleted, supporting surface biodegradation (Peters and Moldowan, 1991). In contrast, tricyclopolyterpanes, diasteranes, and aromatic steroids remain unaltered. Atauri-4 has been ranked at biodegradation level 8, which means that this sample has a depletion of steranes, diasteranes, pregnanes, and triaromatic steroids, though showing a well-defined distribution of triterpanes. Although we cannot preclude other possibilities - mixture of oil charges and/or multiple alteration processes - to account for this anomalous triterpane distribution, exceptionally there are modifications in the usual order of the biodegradation

sequence (Requejo and Halpern, 1989; Bennett and Larter, 2008). Also, the lack of steranes, diasteranes, pregnanes, and triaromatic steroids, as well as the low presence of 17α -hopanes in Maestu-7, indicate a level 9 for biodegradation for this latter sample. In Maestu-1 and Atauri-3, pentacyclic triterpanes, steranes, diasteranes, pregnanes, triaromatic steroids, as well as several tricyclopolyprenanes and monoaromatic steroids, appear to be removed, whereas monoaromatic diasteroids appear to be preserved, which suggests that these two similar samples reach biodegradation level 10.

Rampalay-1 and Rampalay-2 range between biodegradation levels 5 and 6 in the Peters and Moldowan scale, which means that they both have a total absence of isoprenoids, *n*-alkanes, phenanthrenes, dibenzothiophenes, and 25-norhopanes, whereas steranes, hopanes and more highly recalcitrant compounds have not been significantly affected in these two samples.

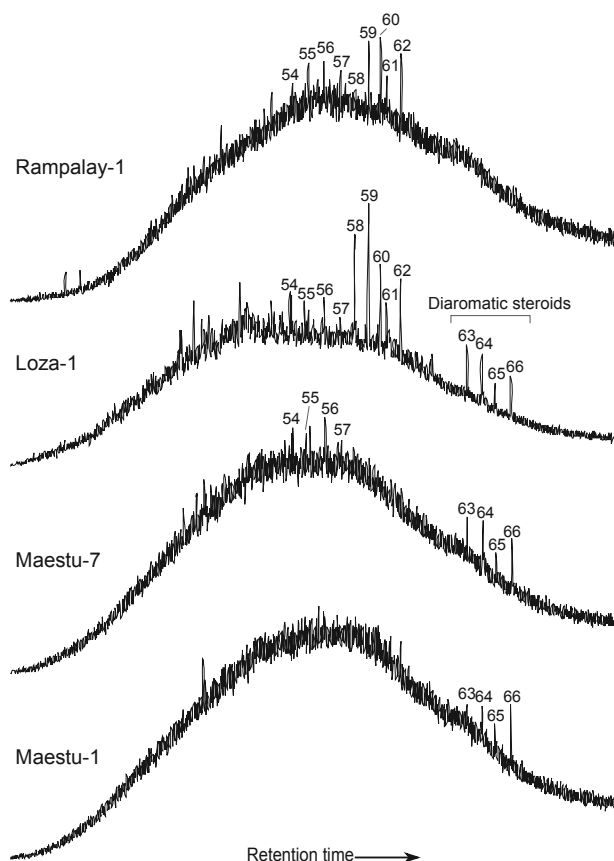


FIGURE 5. Gas chromatograms of the aromatic fractions of the western tar sands (Rampalay-1) and three progressively more biodegraded eastern oil shows (Loza-1, Maestu-7 and Maestu-1). Compounds are listed in Table 1.

Thermal maturity

The hopane isomerization ratios for Atauri-4 (%22S, Table 3) show nearly identical values (approx. 0.6), which is indicative of a thermal maturity level within the oil window (Mackenzie and Maxwell, 1981). Nevertheless, these values must be interpreted with caution due to the fact that %22S and other parameters are known to be altered by biodegradation (Peters *et al.*, 2005). MA(I)/MA(I+II) can also be used to determine the level of maturity reached by organic matter (Seifert and Moldowan, 1978). MA(I) and MA(II) here are defined as the whole contents of C_{21} plus C_{22} monoaromatic steroids and the sum of all C_{27} to C_{29} , respectively. Values on the order of 50% for Atauri-4 and Maestu-7 (see Table 3) are indicative of materials generated from kerogens covering a maturity range close to maximum peak oil generation (Hunt, 1996). The TA ratio is useful as a maturity parameter for Loza-1 and Loza-3 as well. This indicator is defined as the ratio of C_{20} triaromatic steroid relative to the sum of C_{20} and C_{28} 20R triaromatic steroids (Peters *et al.*, 2005). These latter two samples show similar MA(I)/MA(I+II) ratios (~40%), TA ratios (~61%), and calculated equivalent vitrinite reflectances (VRE) around 0.8%. These results reveal slightly low maturation levels of Loza-1 and Loza-3 asphaltic oils when compared to those of Atauri-4 and Maestu-7 (see Table 3). The predominance of ETIO vanadyl-porphyrins over VO-DPEP (PMP or Porphyrin Maturity Parameter values - defined as the ratio of C_{28} ETIO to C_{32} DPEP - about 100%) in the six eastern samples supports a thermal maturity level of at least 0.8%, even with severe biodegradation (Sundararaman *et al.*, 1988; Sundararaman and Hwang, 1993). This is consistent with previous work reporting that the western Basque-Cantabrian oil shows reached thermal maturity levels of VRE of about 0.8% (Beroiz and Permanyer, 2011).

Depositional environment and source rock type

Several molecular parameters have been determined for the asphaltic oils from Álava to establish sedimentary depositional environment, source rock or type of organic matter (see Table 4). However, the Maestu-1, Maestu-7, and Atauri-3 samples suffered such severe biodegradation that they exhibit no recognizable free regular steranes, diasteranes and extended hopanes, among others.

Loza-1 and Loza-3 display low diasterane contents and, consequently, low diasterane-to-sterane ratios (0.09 on average), suggesting that both samples were generated from organic matter deposited in a predominantly carbonate environment under reducing conditions (Peters *et al.*, 2005). By contrast, Rampalay tar sands and the Cordovilla source rock display over 0.56 diasterane ratios,

suggesting that these latter oil shows were derived from a shaly-siliciclastic source rock (Grantham and Wakefield, 1988). In this sense, the plot of the C_{29} to C_{30} hopanes ratio ($C_{29}H/C_{30}H$) versus the C_{35} to $C_{34}22S$ hopane ratio ($C_{35}22S/C_{34}22S$) can be used as a paleodepositional-environmental indicator of sedimentary rocks (Peters *et al.*, 2005). As shown in Figure 7A, Atauri-4 lies within the reducing/carbonate zone, showing a high value of 30-norhopane/hopane, whereas the three aforementioned

western Basque-Cantabrian oil shows lie within the oxic-dysoxic/shaly-siliciclastic zone, presenting $C_{29}H/C_{30}H$ values lower than 0.6 and $C_{35}22S/C_{34}22S$ lower than one. Additionally, Loza-1, Loza-3, Maestu-7, and Atauri-4 samples show T_s to T_m ratios (T_s/T_m) lower than one, suggesting that these samples were probably derived from a carbonate source rock deposited in a reducing environment (McKirby *et al.*, 1983; Rullkötter *et al.*, 1985). By contrast, the western Basque-Cantabrian

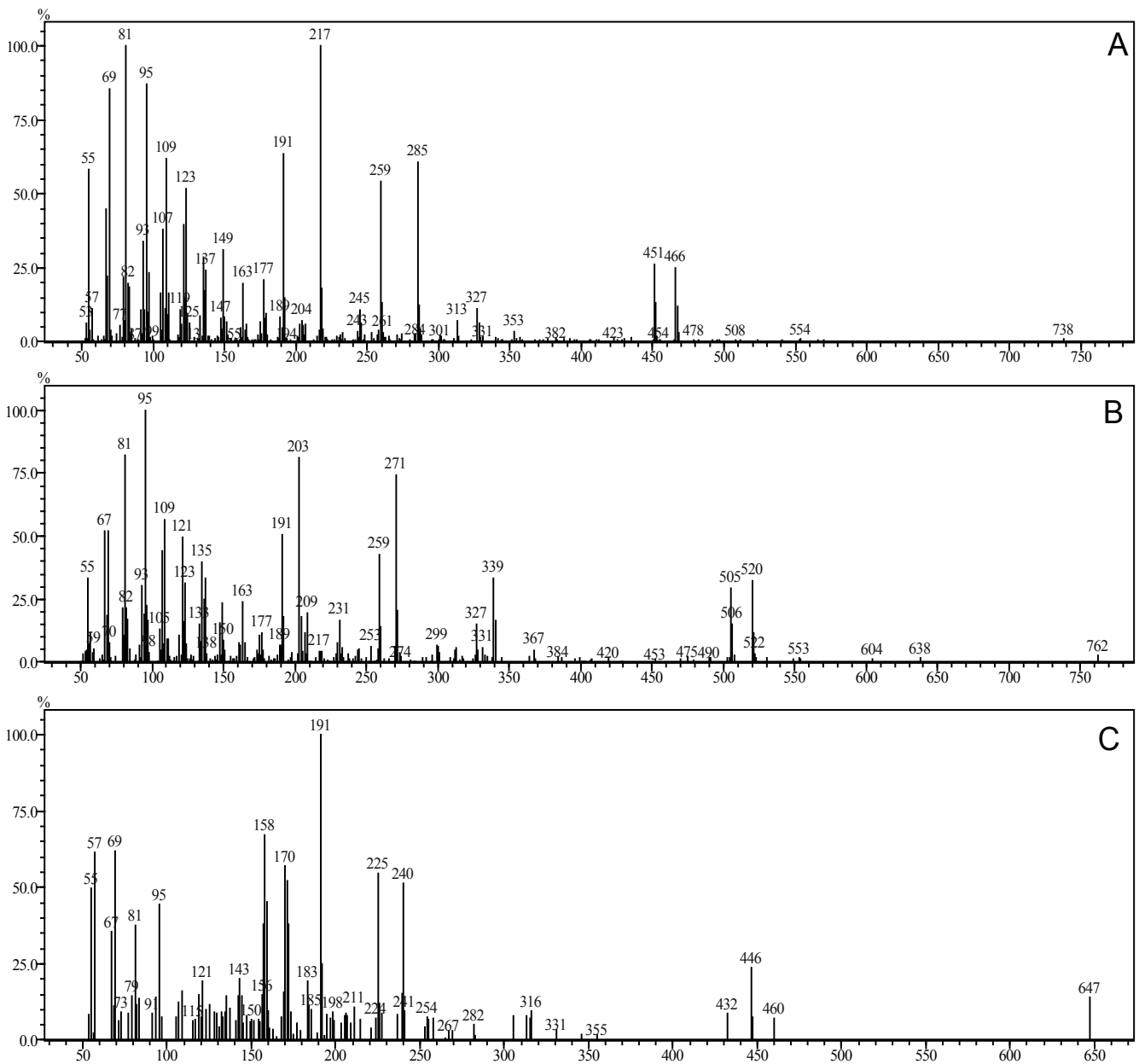


FIGURE 6. Characteristic mass spectra of the three series of compounds eluting at high retention times: A) C_{33} to C_{39} hexacyclic triterpenoids, B) C_{36} to C_{38} heptacyclic alkanes, C) C_{31} to C_{34} diaromatic hydrocarbons.

oil shows present Ts/Tm ratios over one, which may indicate oxic-disoxic conditions (McKirdy *et al.*, 1984). Despite the fact that Ts/Tm can be influenced by maturity (Peters *et al.*, 2005), it can be stated that calculated vitrinite reflectances for all the study asphaltic oils from the Basque-Cantabrian Basin are in the 0.8–0.9% range (Beroiz and Permanyer, 2011).

It is also noteworthy that there is a high abundance of gammacerane in several samples from the eastern part of the Basque-Cantabrian Basin, which may be indicative of oil shows deriving from organic matter deposited in a water-stratified depositional environment (Sinninghe-Damsté *et al.*, 1995). Loza-1, Loza-3, Maestu-7, Maestu-1, and Atauri-3 have very high values of the gammacerane index (see Table 4), which may be explained by the fact that gammacerane is more recalcitrant than 17 α -hopane (Peters *et al.*, 2005). Thus, these high values are not conclusive. However, Atauri-4 shows a gammacerane index of about 0.4, and this value is high enough to suggest an oxygen-poor water-stratified depositional environment for this sample (Dorronsoro *et al.*, 1994). Lastly, as expected, the oil shows from Rampalay and Cordovilla (see Table 4) display significantly lower gammacerane indices (averaging 0.08) than Atauri-4.

The particularly high abundance of pregnane homologues in Loza-1 and Loza-3 may denote water

column stratification or a hypersaline environment (ten Haven *et al.*, 1985). However, it has been reported (Connan, 1984; Peters *et al.*, 2005) that the pregnane-to-sterane ratio can be modified by biodegradation (pregnanes are generally more recalcitrant than regular steranes and C₂₉ regular steranes are slightly degraded in both samples) and by thermal maturity (thermal stabilities for pregnanes are higher than those for regular steranes).

The Rampalay tar sands and the Cordovilla source rock show the same sterane distribution (see Fig. 7B), which is attributed to planktonic marine depositional environments in many cases (Huang and Meinschein, 1979; Moldowan *et al.*, 1985).

Taking into account that all samples from Álava reach high biodegradation levels, it should be pointed out that it is difficult to establish their type of organic matter and depositional environment (Talukdar *et al.*, 1986). However, V/(Ni+V) values on the order of 0.45 for these six samples may indicate a marine-lagoonal transitional environment under low-oxygen conditions (Lewan, 1984). In this sense, despite the concentrations of V and Ni can be influenced by biodegradation, the V/(Ni+V) ratio itself tends to be constant due to the structural similarities among organometallic compounds that contain both metals (Lewan and Maynard, 1982). Also, samples from the eastern part of the basin show a significant presence of

TABLE 3. Maturity-related indices for the hydrocarbons from the Álava sector (eastern Basque-Cantabrian Basin)

Sample	Preg/St ^a	Dia/St ^b	C ₂₉ /C ₃₀ hopanes	GammIndex ^c
Atauri-3	-	-	1.84 ^d	0.82 ^d
Atauri-4	-	-	0.77	0.39
Loza-1	0.36	0.07	2.17 ^d	0.82 ^d
Loza-3	0.43	0.11	2.82 ^d	0.92 ^d
Maestu-1	-	-	0.91 ^d	0.98 ^d
Maestu-7	-	-	1.84 ^d	0.86 ^d
Rampalay-1	0.22	0.67	0.44	0.09
Rampalay-2	0.23	0.69	0.46	0.09
Cordovilla	0.14 ^e	0.57 ^e	0.41 ^e	0.06 ^e

^aPreg/St = (C₂₁+C₂₂)/(C₂₁+C₂₂+C₂₉ $\alpha\alpha\alpha$ S+C₂₉ $\alpha\beta\beta$ R+C₂₉ $\alpha\beta\beta$ S+C₂₉ $\alpha\alpha\alpha$ R).

^bDia/St = (C₂₇ $\beta\alpha$ S+C₂₇ $\beta\alpha$ R)/(C₂₇ $\beta\alpha$ S+C₂₇ $\beta\alpha$ R+C₂₉ $\alpha\alpha\alpha$ S+C₂₉ $\alpha\beta\beta$ R+C₂₉ $\alpha\beta\beta$ S+C₂₉ $\alpha\alpha\alpha$ R).

^cGammIndex = Gamm/(Gamm+C₃₀H).

^dValue affected by partial loss of some biomarker(s).

^eData from Beroiz and Permanyer (2011)

TABLE 4. Source-related indices for the eastern oil shows (Atauri, Loza and Maestu) and western hydrocarbons (Rampalay tar sands and Cordovilla source rock)

Sample	Preg/St ^a	Dia/St ^b	C ₂₉ /C ₃₀ hopanes	GammIndex ^c
Atauri-3	-	-	1.84 ^d	0.82 ^d
Atauri-4	-	-	0.77	0.39
Loza-1	0.36	0.07	2.17 ^d	0.82 ^d
Loza-3	0.43	0.11	2.82 ^d	0.92 ^d
Maestu-1	-	-	0.91 ^d	0.98 ^d
Maestu-7	-	-	1.84 ^d	0.86 ^d
Rampalay-1	0.22	0.67	0.44	0.09
Rampalay-2	0.23	0.69	0.46	0.09
Cordovilla	0.14 ^e	0.57 ^e	0.41 ^e	0.06 ^e

^aPreg/St= (C₂₁+C₂₂)/(C₂₁+C₂₂+C₂₉αααS+C₂₉αββR+C₂₉αββS+C₂₉αααR).

^bDia/St= (C₂₇βαS+C₂₇βαR)/(C₂₇βαS+C₂₇βαR+C₂₉αααS+C₂₉αββR+C₂₉αββS+C₂₉αααR).

^cGammIndex= Gamm/(Gamm+C₃₀H).

^dValue affected by partial loss of some biomarker(s).

^eData from Beroiz and Permanyer (2011)

ETIO and DPEP vanadyl-porphyrins, which may denote a marine to mixed marine/terrestrial organic matter source and oxygen-deprived conditions of sediment deposition (Sundadaran and Raedeke, 1993).

Geochemical correlations

The relative abundance of C₂₇, C₂₈ and C₂₉ monoaromatic steroids is a valid oil-to-oil and oil-to-source rock correlation tool (Peters *et al.*, 2005). Then, the ternary plot of C₂₇, C₂₈ and C₂₉ 5β10β-20S monoaromatic steroids (Fig. 7C) suggests that the two Rampalay tar sands have a different precursor organic matter when compared with the samples from Álava. Furthermore, a statistical treatment based on 12 parameters (% Sat, % Aro, % Asp, δ¹³C_{sat}, δ¹³C_{aro}, δ¹³C_{asp}, δ¹³C^{whole} oil, VRE, V/Ni, Ni concentration, GammIndex and C₂₉/C₃₀ hopanes) was made by means of hierarchical clustering in order to classify all the samples into one or more groups (Fig. 8). The Euclidean distance was used as a grouping parameter (Romesburg, 1984). As expected, the dendrogram plot in Figure 8 displays four clusters, namely Loza, Atauri, Maestu, and the three western Basque-Cantabrian occurrences. Using the proximity procedure (Everitt,

1993), a calculation through the centroid method shows that these four clusters have a significant degree of dissimilarity.

CONCLUSIONS

Loza-1, Loza-3, Maestu-7, Maestu-1, Atauri-4, and Atauri-3 samples (South-East of the basin) were affected by severe biodegradation processes and reached a thermal maturity level in the VRE 0.8–0.9% range, close to peak oil generation. Also, the six samples from the eastern part of the Basque-Cantabrian Basin appear to be derived from carbonate source rocks deposited under reducing, water-stratified and likely hypersaline conditions that might correspond to a transitional environment. In contrast, tar sands from Rampalay and the Cordovilla source rock (western part of the basin) correlate with the Ayoluengo oils, which were generated in a marine shaly environment. On the whole, the oil shows from exhumed reservoirs in the eastern Basque-Cantabrian Basin (Álava sector) have a different genetic origin when compared to tar sands, source rocks, and oils from the western part of the aforementioned basin.

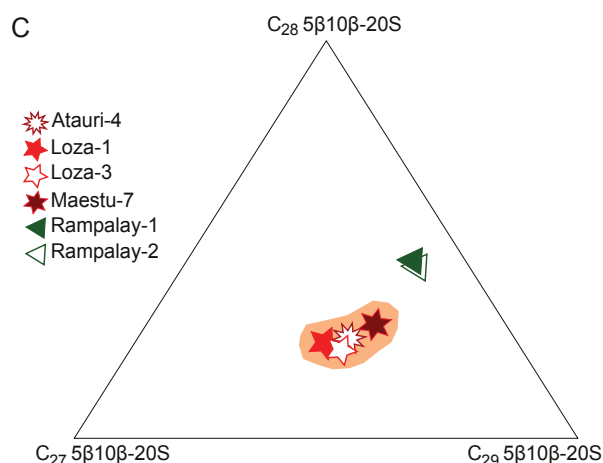
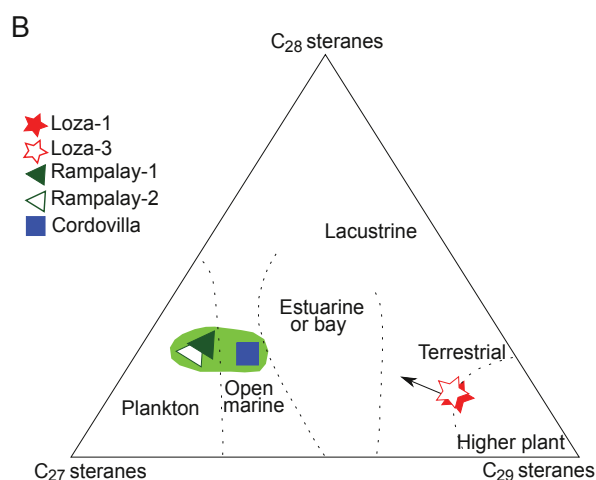
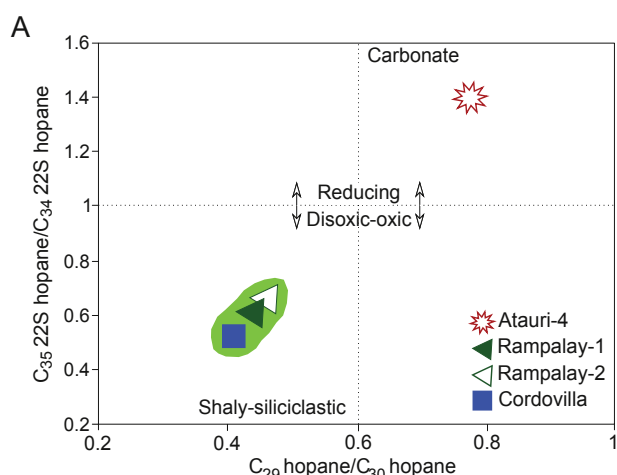


FIGURE 7. Precursor organic matter, source-rock type and depositional environment plots showing the comparison between the western hydrocarbons (Cordovilla source rock and Rampalay tar sands) and the eastern hydrocarbons (Atauri, Loza and Maestu oil shows). A) $C_{29}H/C_{30}H$ vs. $C_{35}22S/C_{34}22S$ plot; B) C_{27} , C_{28} and C_{29} steranes ternary plot. An arrow indicates the biodegradation restoration sense for the Loza samples; C) C_{27} , C_{28} and C_{29} $\beta 5\beta 10-20S$ monoaromatic steroids ternary plot.

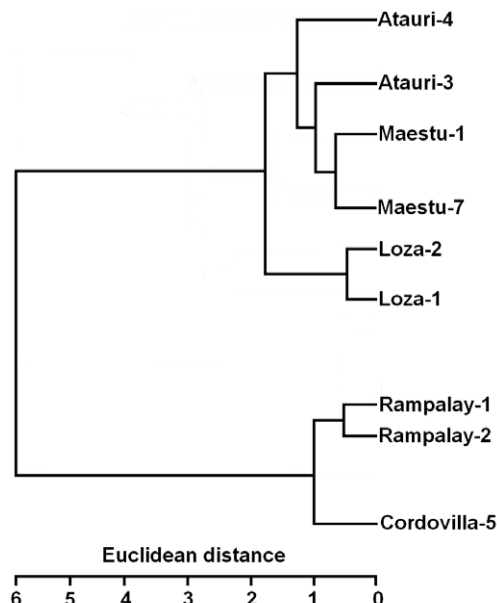


FIGURE 8. Dendrogram showing the clustering of the eastern oil shows and the western Rampalay tar sands and Cordovilla source rock.

ACKNOWLEDGMENTS

This article is part of the “Alago Special Publication: selected contributions from the XIII Congress”. This study was funded by the Ministerio de Ciencia e Innovación (Research Project CGL2010-15887). We also thank the two reviewers (J.A. Curiale and D. García-Bautista) for their comments which helped to improve the original version of this research work.

REFERENCES

Ábalos, B., Alkorka, A., Iríbar, V., 2008. Geological and isotopic constraints on the structure of the Bilbao anticlinorium (Basque–Cantabrian Basin, North Spain). *Journal of Structural Geology*, 30, 1354-1367.

Agirrezabala, L.M., Dorronsoro, C., Permanyer, A., 2008. Geochemical correlation of pyrobitumen fills with host mid-Cretaceous Black Flysch Group (Basque-Cantabrian Basin, western Pyrenees). *Organic Geochemistry*, 39, 1185-1188.

Alonso, J.L., Pulgar, J.A., Pedreira, D., 2007. El relieve de la Cordillera Cantábrica. *Enseñanza de las Ciencias de la Tierra*, 15(2), 151-163.

Alonso-Zarza, A.M., Armenteros, I., Braga, J.C., Muñoz, A., Pujalte, V., Ramos, E., 2002. Tertiary. In: Gibbons, W., Moreno, T. (eds.). *The Geology of Spain*. London, Geological Society, 293-334.

Alvarez de Buergo, E., García, A., 1996. Cálculo de reservas remanentes de hidrocarburos en zonas estructuralmente

- complejas: aplicación al campo de Ayoluengo, 1ª parte. *Geogaceta*, 20, 161-164.
- ASTM, 2004. Standard Test Method for Sediment in Fuel Oils by the Centrifugation Method: Annual Book of the American Society for Testing Materials Standards, v. 05.01 and 05.02. West Conshohocken, Pennsylvania, ASTM International.
- Barnolas, A., Pujalte, V., 2004. La cordillera Pirenaica. In: Vera, J.A. (ed). *Geología de España*. Madrid, Sociedad Geográfica Española-Instituto Geológico y Minero de España, 231-344.
- Bennett, B., Larter, S., 2000. Quantitative separation of aliphatic and aromatic hydrocarbons using silver ion-silica solid-phase extraction. *Analytical Chemistry*, 72(5), 1039-1044.
- Bennett, B., Larter, S.R., 2008. Biodegradation scales: applications and limitations. *Organic Geochemistry*, 39, 1222-1228.
- Bennett, B., Fustic, M., Farrimond, P., Huang, H., Larter, S.R., 2006. 25-Norhopanes: Formation during biodegradation of petroleum in the subsurface. *Organic Geochemistry*, 37(7), 787-797.
- Beroiz, C., Permanyer, A., 2011. Hydrocarbon habitat of the Sedano Trough, Basque-Cantabrian Basin, Spain. *Journal of Petroleum Geology*, 34(4), 387-410.
- Cámara, P., 1997. The Basque Cantabrian Basin, Mesozoic tectono-sedimentary evolution. *Mémoires de la Société Géologique de France*, 171, 187-191.
- Capote, R., Muñoz, J.A., Simón, J.L., Liesa, C.L., Arlegui, L.E., 2002. Alpine Tectonics I. The Alpine System north of the Betic Cordillera. In: Gibbons, W., Moreno, T. (eds.). *The Geology of Spain*. London, Geological Society, 367- 400.
- Carreras-Suárez, F., Ramírez del Pozo, J., 1978. Mapa y memoria explicativa de la Hoja de Eulate (139) del Mapa geológico de España a escala 1:50.000. Madrid, Instituto Geológico y Minero de España, 36pp.
- Connan, J., 1984. Biodegradation of crude oils in reservoirs. In: Brooks, J., Welte, D. (eds.). *Advances in Petroleum Geochemistry*, Vol. 1. London, Academic Press, 299-335.
- Cooper, B.S., Barnard, P.C., 1984. Source-rock and oils of the Central and Northern North Sea. In: Demaison, G., Murriss, R.J. (eds.). *Petroleum Geochemistry and Basin Evaluation*. Tulsa, American Association of Petroleum Geologists, 35, 303-314.
- Dorronsoro, C., García, M.R., Grimalt, J.O., 1994. Triterpane distribution in diapir-related asphalts. *Fuel*, 73, 83-91.
- Everitt, B.S., 1993. *Cluster Analysis*. New York, John Wiley & Sons Inc., 170pp.
- Galimov, E.M., 2006. Isotope organic geochemistry. *Organic Geochemistry*, 37, 1200-1262.
- Galimov, E.M., Frik, M.G., 1985. Isotopic method of detection of oil source deposits. *Geokhimiya*, 10, 1474-1485.
- García Sánchez, M.R., 1994. Caracterización geoquímica de bitúmenes naturales en torno al diapiro de Maestu (Álava). Análisis de asfaltenos y resinas. Doctoral Thesis. Universitat de Barcelona, 249pp.
- Gómez, M., Vergés, J., Riaza, C., 2002. Inversion tectonics of the Northern margin of the Basque Cantabrian Basin. *Bulletin de la Société Géologique de France*, 173, 49-59.
- Gräfe, K.U., Wiedmann, J., 1993. Sequence stratigraphy in the Upper Cretaceous of the Basco-Cantabrian Basin (northern Spain). *Geologische Rundschau*, 82, 327-361.
- Grantham, P.J., Wakefield, L.L., 1988. Variations in the sterane carbon number distributions of marine source rocks derived crude oils through geological time. *Organic Geochemistry*, 12, 61-73.
- Herron, S.L., Le Tendre, L., 1990. Wireline source rock evaluation in the Paris Basin. In: Huc, A.Y. (ed.). *Deposition of Organic Facies*. Studies in Geology. Tulsa, American Association of Petroleum Geologists, 30, 57-72.
- Huang, W.Y., Meinschein, W.G., 1979. Sterols as ecological indicators. *Geochimica et Cosmochimica Acta*, 43, 739-745.
- Huc, A.Y., 1990. Understanding organic facies: a key to improved quantitative petroleum evaluation of sedimentary basins. In: Huc, A.Y. (ed.). *Deposition of Organic Facies*. Studies in Geology. Tulsa, American Association of Petroleum Geologists, 30, 1-12.
- Hunt, M., 1996. *Petroleum Geochemistry and Geology*, 2nd Edition. New York, Freeman Editions, 743pp.
- Lewan, M.D., 1984. Factors controlling the proportionality of vanadium to nickel in crude oils. *Geochimica et Cosmochimica Acta*, 48, 2231-2238.
- Lewan, M.D., Maynard, J.B., 1982. Factors controlling enrichment of vanadium and nickel in the bitumen of organic sedimentary rocks. *Geochimica et Cosmochimica Acta*, 46, 2547-2560.
- Li, M., Riediger, C.L., Fowler, M.G., Snowdon, L.R., Abrajano JR, T.A., 1996. Unusual polycyclic alkanes in Lower Cretaceous Ostracode Zone sediments and related oils of the Western Canada sedimentary basin. *Organic Geochemistry*, 25(3/4), 199-209.
- Mackenzie, A.S., Maxwell, J.R., 1981. Assessment of thermal maturation in sedimentary rocks by molecular measurements. In: Brooks, J. (ed.). *Organic Maturation Studies and Fossil Fuel Exploration*. London, Academic Press, 239-254.
- Mansuy, L., Philp, R.P., Allen, J., 1997. Source identification of oil spills based on the isotopic composition of individual components in weathered oil samples. *Environmental Science and Technology*, 31, 3417-3425.
- Marín, P., 2002. Caracterización geoquímica de los hidrocarburos en reservorios exhumados de la Cuenca Vasco-Cantábrica. MSc Thesis. Universitat de Barcelona, 23pp.
- McKirdy, D.M., Aldridge, A.K., Ypma, P.J.M., 1983. A geochemical comparison of some crude oils from Pre-Ordovician carbonate rocks. In: Albrecht, P., Bjorøy, M., Cornford, C., de Groot, K., Eglinton, G., Galimov, E., Laythaeuser, D., Pelet, R., Rullkötter, J., Speers, G. (eds.). *Advances in Organic Geochemistry*, 1981. Chichester, John Wiley & Sons Inc., 99-107.
- McKirdy, D.M., Kantsler, A.J., Emmett, J.K., Aldridge, A.K., 1984. Hydrocarbon genesis and organic facies in Cambrian carbonates of the Eastern Officer Basin, South Australia. In: Palacas, J.G., (ed.). *Petroleum Geochemistry and Source Rock Potential of Carbonate Rocks*. Tulsa, American Association of Petroleum Geologists, 13-31.

- Meckenstock, R.U., Morasch, B., Warthmann, R., Schink, B., Annweiler, E., Michaelis, W., Richnow, H.H., 1999. 13C/12C isotope fractionation of aromatic hydrocarbons during microbial degradation. *Environmental Microbiology*, 1, 409-414.
- Moldowan, J.M., Fago, F.J., 1986. Structure and significance of a novel rearranged monoaromatic steroid hydrocarbon in petroleum. *Geochimica et Cosmochimica Acta*, 50, 343-351.
- Moldowan, J.M., Seifert, W.K., Gallegos, E.J., 1985. Relationship between petroleum composition and depositional environment of petroleum source rocks: Tulsa, American Association of Petroleum Geologists Bulletin, 69, 1255-1268.
- Permanyer, A., Márquez, G., Gallego, J.R., 2013. Compositional variability in oils and formation waters from the Ayoluengo and Hontomín fields (Burgos, Spain). Implications for assessing biodegradation and reservoir compartmentalization. *Organic Geochemistry*, 54, 125-139.
- Peters, K.E., Moldowan, J.M., 1991. Effects of source, thermal maturity and biodegradation on the distribution and isomerization of homohopanes in petroleum. *Organic Geochemistry*, 17, 47-61.
- Peters, K.E., Walters, C.C., Moldowan, J.M., 2005. The Biomarker Guide, Vol. 2: Biomarkers and Isotopes in Petroleum Systems and Earth History, 2nd edition. Cambridge, Cambridge University Press, 1132pp.
- Poinsot, J., Dessort, D., Adam, P., Lacrampe, G., Trendel, J.M., Albrecht, P., 1995. New and rare biomarkers: saturated C33-C43 polycycloisoprenoids. In: Dorronsoro, C., Grimalt, J.O. (eds.). *Organic Geochemistry: Developments and Applications to Energy, Climate, Environment and Human History*. Donostia-San Sebastian, AIGOA, 116-118.
- Portero, J.M., Ramírez del Pozo, J., 1979. Mapa y memoria explicativa de la Hoja de Haro (170) del Mapa geológico de España a escala 1:50.000. Madrid, Instituto Geológico y Minero de España, 43pp.
- Pujalte, V., 1977. El complejo Purbeck-Wealden de Santander. Estratigrafía y sedimentación. Doctoral Thesis. Universidad del País Vasco, 202pp.
- Quesada, S., Robles, S., Rosales, I., 2005. Depositional architecture and transgressive-regressive cycles within Lias backstepping carbonate ramps in the Basque-Cantabrian Basin, northern Spain. *Journal of the Geological Society*, 162, 531-548.
- Quesada, S., Dorronsoro, C., Robles, S., Chaler, R., Grimalt, J.O., 1997. Geochemical correlation of oil from Ayoluengo field to Liassic black shale units in the southwestern Basque-Cantabrian Basin (northern Spain). *Organic Geochemistry*, 27, 25-40.
- Ramírez del Pozo, J., 1969. Síntesis estratigráfica y micropaleontológica de las facies Purbeck y Wealdense del Norte de España. Madrid, Ediciones CEPESA S.A., 68pp.
- Rat, R., 1988. The Basque-Basque-Cantabrian Basin between the Iberian and European plates: Some facts but still many problems. *Revista de la Sociedad Geológica de España*, 1, 327-348.
- Requejo, A.G., Halpern, H.I., 1989. An unusual hopane biodegradation sequence in tar sands from the Pt Arena (Monterey) Formation. *Nature*, 342, 670-673.
- Riolo, J., Hussler, G., Albrecht, P., Connan, J., 1986. Distribution of aromatic steroids in geological samples: their evaluation as geochemical parameters. *Organic Geochemistry*, 10, 981-990.
- Roest, W.R., Srivastava, S.P., 1991. Kinematics of the plate boundaries between Eurasia, Iberia and Africa in the North Atlantic from the Late Cretaceous to the present. *Geology*, 19, 613-616.
- Romesburg, H.C., 1984. Cluster Analysis for researches. Belmont, Lifetime Learning Publications, 334pp.
- Rullkötter, J., Spiro, B., Nissenbaum, A., 1985. Biological marker characteristics of oils and asphalts from carbonate source rocks in a rapidly subsiding graben, Dead Sea, Israel. *Geochimica et Cosmochimica Acta*, 49, 1357-1370.
- Salamon, J., 1982. Les formations continentales du Jurassique Supérieur-Crétacé Inférieur (Espagne du Nord. Chaînes Cantabrique et NW Ibérique). Dijon, Mémoires Géologiques de l'Université de Dijon, 6, 227pp.
- Sanz, R., 1967. The Ayoluengo Field. Seventh World Petroleum Congress Proceedings, 2, 251-258.
- Seifert, W.K., Moldowan, J.M., 1978. Application of steranes, terpanes and monoaromatic to the maturation, migration and source of crude oils. *Geochimica et Cosmochimica Acta*, 42, 77-95.
- Seifert, W.K., Moldowan, J.M., Demaison, G.J., 1984. Source correlation of biodegraded oils. *Organic Geochemistry*, 6, 633-643.
- Sinninghe-Damsté, J.S., Kenig, F., Koopmans, M.P., Köster, J., Schouten, S., Hayes, J.M., de Leeuw, J.W., 1995. Evidence for gammacerane as an indicator of water-column stratification. *Geochimica et Cosmochimica Acta*, 59, 1895-1900.
- Sofer, Z., 1984. Stable Carbon Isotope composition of crude oils: application to source depositional environments and petroleum alteration. *The American Association of Petroleum Geologists Bulletin*, 68, 31-49.
- Sundararaman, P., 1985. High-performance liquid chromatography of vanadyl porphyrins. *Analytical Chemistry*, 57, 2204-2206.
- Sundararaman, P., Hwang, R.J., 1993. Effect of biodegradation on vanadyl porphyrin distribution. *Geochimica et Cosmochimica Acta*, 57, 2283-2290.
- Sundararaman, P., Raedeke, L.D., 1993. Vanadyl porphyrins in exploration: maturity indicators for source rocks and oils. *Applied geochemistry*, 8, 245-254.
- Sundararaman, P., Biggs, W.R., Reynolds, J.G., Fetzer, J.C., 1988. Vanadyl porphyrins, indicators of kerogen breakdown and generation of petroleum. *Geochimica et Cosmochimica Acta*, 52, 2337-2341.
- Talukdar, S.C., Gallango, O., Chin-A-Lien, M., 1986. Generation and migration of hydrocarbons in the Maracaibo Basin,

- Venezuela: an integrated basin study. *Organic Geochemistry*, 10, 261-279.
- ten Haven, H.L., de Leeuw, J.W., Schenck, P.A., 1985. Organic geochemical studies of a Messinian evaporitic basin, Northern Appenines (Italy) I: hydrocarbon biological markers for a hypersaline environment. *Geochimica et Cosmochimica Acta*, 49, 2181-2191.
- Tissot, B. and Welte, D.H., 1984. *Petroleum formation and occurrence*, 2nd edition. Berlin, Springer-Verlag, 699pp.

Manuscript received March 2014;
revision accepted September 2014;
published Online October 2014.

APPENDIX

TABLE I. Triterpanes, steranes and aromatics compounds identified in the total ion chromatograms and fragmentograms

1	C ₁₉ tricyclic terpane	38	C ₃₆ heptacyclic alkane
2	C ₂₀ tricyclic terpane	39	C ₃₈ hexacyclic alkane
3	C ₂₁ tricyclic terpane	40	C ₃₉ hexacyclic alkane
4	C ₂₂ tricyclic terpane	41	C ₃₇ heptacyclic alkane
5	C ₂₃ tricyclic terpane	42	C ₃₈ heptacyclic alkane
6	C ₂₄ tricyclic terpane	43	5 α (H), 14 α (H), 17 α (H)-pregnane (pregnane)
7	C ₂₅ tricyclic terpane	44	5 α (H), 14 β (H), 17 β (H)-pregnane (diginane)
8	C ₂₄ tetracyclic terpane	45	20-methyl-5 α (H), 14 α (H), 17 α (H)-pregnane (homopregnane)
9a	C ₂₆ tricyclic terpane 17R	46	20-methyl-5 α (H), 14 β (H), 17 β (H)-pregnane (homodiginane)
9b	C ₂₆ tricyclic terpane 17S	47	13 β (H), 17 α (H)-diacholestane 20S
10a	C ₂₈ tricyclic terpane 17R	48	13 β (H), 17 α (H)-diacholestane 20R
10b	C ₂₈ tricyclic terpane 17S	49a	5 α (H), 14 α (H), 17 α (H)-cholestane 20S*
11a	C ₂₉ tricyclic terpane 17R	49b	5 α (H), 14 β (H), 17 β (H)-cholestane 20R*
11b	C ₂₉ tricyclic terpane 17S	49c	5 α (H), 14 β (H), 17 β (H)-cholestane 20S*
12	18 α (H)-22,29,30-trisnorhopane	49d	5 α (H), 14 α (H), 17 α (H)-cholestane 20R
13	17 α (H)-22,29,30-trisnorhopane	50	24-ethyl-13 β (H), 17 α (H)-diacholestane 20R
14a	C ₃₀ tricyclic terpane 17R	51a	24-methyl-5 α (H), 14 α (H), 17 α (H)-cholestane 20S
14b	C ₃₀ tricyclic terpane 17S	51b	24-methyl-5 α (H), 14 β (H), 17 β (H)-cholestane 20R*
15	17 α (H), 21 β (H)-30-norhopane	51c	24-methyl-5 α (H), 14 β (H), 17 β (H)-cholestane 20S
16	18 α (H)-30-norhopane	51d	24-methyl-5 α (H), 14 α (H), 17 α (H)-cholestane 20R
17	15 α -methyl-17 α (H)-27-norhopane (diahopane)	52a	24-ethyl-5 α (H), 14 α (H), 17 α (H)-cholestane 20S
18	17 β (H)-21 α (H)-30-norhopane (normoretane)	52b	24-ethyl-5 α (H), 14 β (H), 17 β (H)-cholestane 20R
19	17 α (H), 21 β (H)-hopane	52c	24-ethyl-5 α (H), 14 β (H), 17 β (H)-cholestane 20S
20	17 β (H), 21 α (H)-hopane (moretane)	52d	24-ethyl-5 α (H), 14 α (H), 17 α (H)-cholestane 20R
21a	17 α (H), 21 β (H)-homohopane 22S	53a	24-propyl-5 α (H), 14 α (H), 17 α (H)-cholestane 20S
21b	17 α (H), 21 β (H)-homohopane 22R	53b	24-propyl-5 α (H), 14 β (H), 17 β (H)-cholestane 20R
22	Gammacerane	53c	24-propyl-5 α (H), 14 β (H), 17 β (H)-cholestane 20S
23a	17 α (H), 21 β (H)-bishomohopane 22S	53d	24-propyl-5 α (H), 14 α (H), 17 α (H)-cholestane 20R
23b	17 α (H), 21 β (H)-bishomohopane 22R	54	5 β (H)-C ₂₇ monoaromatic steroid 20S + C ₂₇ MA diasteroid 20S ^a
24a	17 α (H), 21 β (H)-trishomohopane 22S	55	5 β (H)-C ₂₇ monoaromatic steroid 20R + C ₂₇ MA diasteroid 20R ^a
24b	17 α (H), 21 β (H)-trishomohopane 22R	56	5 β (H)-C ₂₈ monoaromatic steroid 20S + C ₂₈ MA diasteroid 20S ^a
25a	17 α (H), 21 β (H)-tetrakishomohopane 22S	57	5 β (H)-C ₂₈ monoaromatic steroid 20R + C ₂₈ MA diasteroid 20R ^a
25b	17 α (H), 21 β (H)-tetrakishomohopane 22R	58	C ₂₆ triaromatic steroid 20S
26a	17 α (H), 21 β (H)-pentakishomohopane 22S	59	C ₂₆ triaromatic steroid 20R + C ₂₇ triaromatic steroid 20S
26b	17 α (H), 21 β (H)-pentakishomohopane 22R	60	C ₂₈ triaromatic steroid 20S
27	C ₃₃ hexacyclic alkane	61	C ₂₇ triaromatic steroid 20R
28	C ₃₃ hexacyclic alkane	62	C ₂₈ triaromatic steroid 20R
29	C ₃₄ hexacyclic alkane	63	C ₃₁ diaromatic steroid
30	C ₃₄ hexacyclic alkane	64	C ₃₂ diaromatic steroid
31	C ₃₄ hexacyclic alkane	65	C ₃₃ diaromatic steroid
32	C ₃₄ hexacyclic alkane	66	C ₃₄ diaromatic steroid
33	C ₃₅ hexacyclic alkane		
34	C ₃₅ hexacyclic alkane		
35	C ₃₅ hexacyclic alkane		
36	C ₃₆ hexacyclic alkane		
37	C ₃₇ hexacyclic alkane		

^aPeak co-elution